

LUNAR REMNANT MAGNETIC FIELD MAPPING FROM ORBITAL OBSERVATIONS OF MIRRORED ELECTRONS*

J. E. McCOY

NASA/Johnson Space Center, Houston, Tex., U.S.A.

and

K. A. ANDERSON, R. P. LIN, H. C. HOWE, and R. E. McGUIRE

Space Sciences Laboratory, University of California, Berkeley, Calif., U.S.A.

Abstract. Areas of lunar surface magnetic field are observed to 'mirror' low energy electrons present in the normal lunar space environment. The ambient electrons provide, in effect, a probe along the ambient magnetic field lines down to the lunar surface for remote sensing of the presence of surface fields. This probe, unlike direct measurement by the magnetometer, does not require low altitude or a very stable (magnetotail) ambient field to provide a mapping of regions of occurrence of such fields. Use of the on-board vector magnetometer measurements of the ambient magnetic field orientation allows accurate projection of such mapping onto the lunar surface. Preliminary maps of the lunar surface magnetic areas underlying the orbit of the 'Particles and Fields Satellite deployed from Apollo-16' have been generated, obtaining 40% coverage from partial data to demonstrate feasibility of the technique. As well as providing independent verification of areas such as Van de Graaff already discovered in the magnetometer data, these maps reveal many previously unreported areas of surface magnetism. The method is sensitive to fields of less than 0.1γ at the surface. Application to the full body of available PFS-1 & 2 electron data is expected to provide complete mapping of the lunar surface for areas of magnetization up to latitudes of 35–40 deg. The surface field regions observed are generally due to sources smaller than 10–50 km in size, although many individual regions are often so close together as to give much larger regions of effectively continuous mirroring. Absence of consistent mirroring by any global field places an upper limit on the size of any net lunar dipole moment of less than $10^{10}\gamma$ km³. Much additional information regarding the magnetic regions can be obtained by correlated analysis of both the electron return and vector magnetometer measurements at orbital altitude, the two techniques providing each other with directly complimentary measurements at the satellite and along the ambient field lines to the surface.

A significant result of the Apollo program has been the discovery of numerous and extensive areas of magnetism of lunar origin, often referred to as natural remanent magnetization (NRM). Previous measurements by Luna 10 (Dolginov *et al.*, 1966) and Explorer 35 (Sonett *et al.*, 1967) had shown no evidence of any lunar magnetic field, nor of any significant distortion of the external interplanetary or magnetospheric magnetic fields in the process of their passage through the lunar body (Anderson and Lin, 1969; Van Allen and Ness, 1969). The somewhat unexpected discovery of NRM in the Apollo 11 rock samples (Strangway *et al.*, 1970), followed by measurement of local magnetic fields of tens to hundreds of gammas at several lunar surface magnetometer sites (Dyal *et al.*, 1972) and fields exceeding tenths of a gamma at altitudes

* Paper presented at the Conference on 'Interactions of the Interplanetary Plasma with the Modern and Ancient Moon', sponsored by the Lunar Science Institute, Houston, Texas and held at the Lake Geneva Campus of George Williams College, Wisconsin, between September 30 and October 4, 1974.

up to 100 km by the Apollo subsatellite magnetometers (Coleman *et al.*, 1972) was therefore of great interest, as it provided an additional means of constraining the various models of lunar origin, evolution, composition and surface processes. The mapping of location, extent and intensity of such intrinsic lunar magnetic fields has become a matter of basic interest to our understanding of the Moon.

The primary means of producing such maps to date has been the reduction of data from the orbital magnetometer experiments on the PFS-1 and 2 satellites, left in (nominal) 100 km orbits by Apollo 15 and Apollo 16. Maps have been produced covering about 20% of the lunar surface beneath the ground tracks of these satellites, mostly on the far side of the Moon. Primary limitation on such coverage has come from the necessity to use data mostly from portions of the orbit below 100 km during high latitude magnetotail conditions. This limits the useable data to a few days each month when, due to a peculiarity of the orbital precession, the ground track tends to overlie the same areas of the lunar surface each time. According to Sharp *et al.* (1973), the lunar surface magnetic field at orbital altitudes is undistorted by its plasma environment only in the near-vacuum conditions of the north and south lobes of the Earth's magnetotail. At these times, large features of the lunar surface field can be discerned on individual quiet orbits and smaller features can be analyzed by averaging many orbits over the same ground track. The PFS satellite magnetometer data obtained in the geomagnetic tail have shown that it is feasible to map the lunar remanent magnetism by this method; however, high resolution maps of magnetic features can be obtained only with dual magnetometer surveys to separate temporal and spatial changes in the fields and/or with low altitude data.

A significant new method has recently been exploited to detect lunar surface magnetic field enhancements with a high degree of sensitivity and spatial resolution, by means of the observation of energetic electrons from lunar orbit using a detector sectored to distinguish direction of arrival with respect to the ambient magnetic field and the lunar surface (Anderson *et al.*, 1974; Howe *et al.*, 1974). Areas of lunar surface magnetic field are observed to 'mirror' such low energy electrons normally present in the lunar space environment. It is the purpose of this paper to describe the use of this technique for mapping areas of lunar surface magnetism and to present preliminary maps generated to demonstrate feasibility of the technique.

1. Technique

Areas of lunar surface magnetic field are observed to 'mirror' low energy electrons present in the normal lunar space environment. Electron detectors on the lunar orbiting PFS satellites are sectored to determine direction of arrival of the detected electron fluxes. Electrons 'mirrored' by surface field increases are guided by the external interplanetary or magnetotail magnetic field to arrive at the orbiting satellite from directions forbidden direct access to ambient electron fluxes by the presence of the (lunar) absorbing body. The geometry of the situation is illustrated in Figure 1, which shows the sort of trajectory followed by an electron in the total magnetic field resulting from

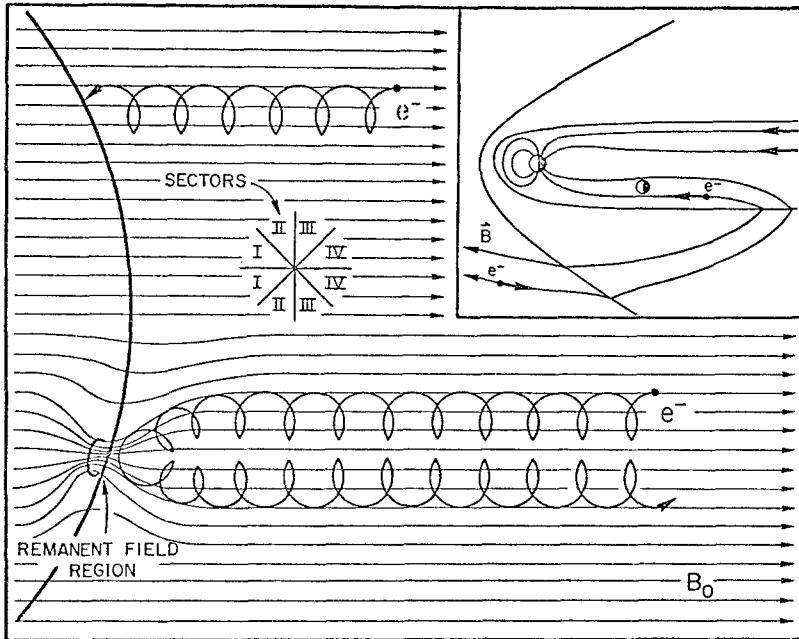


Fig. 1. Illustration of C5 electron analyzer pitch angle sector orientation, and scattering geometry resulting from the combination of a local surface remnant field region with a uniform (external) high latitude magnetotail field. Insert: illustration of access of solar electrons to magnetotail along reconnected field lines.

the superposition of an isolated area of lunar surface magnetism with a uniform external (interplanetary or magnetotail) magnetic field. The regions of intense lunar remnant magnetization discovered by the Apollo 15 and 16 PFS satellite magnetometer (Sharp *et al.*, 1973) were observed to strongly scatter 14 KeV electrons back up the magnetic field lines to arrive at the satellite from directions blocked from direct access by the Moon. Such scattered return (mirrored) electron fluxes have also been observed from numerous other locations on the lunar surface, including many previously unreported. The electrons, in effect, provide a probe along the magnetic field line from orbit to the lunar surface. This probe is sensitive to changes in field strength along its path. If no surface magnetization is present, the electrons are guided by the external magnetic field into the lunar surface where they are absorbed (except for a few percent which are coulomb backscattered and are observed as background flux (Anderson and Lin, 1969).) If surface remnant magnetism is present, the total field strength increases as the electrons enter the region of remnant magnetism, causing a fraction of the electrons to mirror or backscatter with an intensity (which may be observed from orbit returning along the field line from the surface) proportional to the strength and spatial extent of the surface field volume.

Since the energetic electrons needed to serve as field line tracers are always present in the lunar environment (Anderson *et al.*, 1972), this method is useable when the Moon

is in the solar wind as well as when the Moon is in high latitude magnetotail. The primary requirement on stability of the ambient magnetic field is to provide directional reference to the location of intersecting the lunar surface during the period of each measurement (1 to 24 s). Best results are obtained when electron fluxes are high enough ($> 10 \text{ cm}^{-2} \text{ s}^{-1} \text{ ster}^{-1} \text{ KeV}^{-1}$) to give good counting statistics and the external ambient field is oriented within 30° – 40° of perpendicular to the lunar surface (to reduce errors involved in projecting the satellite observed field direction to determine the location of the surface point being observed).

Resolution of the technique is controlled by the gyroradius of the electrons' spiral path along a field line, about 40 km for a 14 keV electron in a typical 10γ external magnetic field. This, coupled with the orbital motion of about 1.6 km s^{-1} , results in a probe averaged over an area roughly 80 km by 120 km for each 24 s data cycle. Resolution of regions on the order of a few kilometers is available from real time data with $\frac{1}{2}$ keV electrons.

If the scale of the remnant field change is large compared to the gyro-radius, electrons of a given pitch angle (α) will be adiabatically mirrored back from any region where B exceeds the value

$$B_m = B \sin^{-2} \alpha, \quad (1)$$

where B and α are the magnetic field strength and pitch angle at the satellite orbit. Therefore, any large scale area of surface remnant field causing as little as 0.1γ increase in the total surface field (B_m) over that remaining at orbital altitude will mirror all incident electrons with pitch angles between 90° – 96° . This would result in observation of a return flux in Sector II (45° – 90°) of about 13% of the incident flux observed in Sector III (90° – 135°), more than twice the background in that sector due to coulomb backscatter from the unmagnetized lunar surface.

If the spatial scale of the remnant magnetism is comparable or smaller than an electron gyro-radius, the electrons will undergo more complex scattering. This will still result in a significant return flux backscattered up the field line, if the region is of sufficient strength and volume to turn the electron's path upward before it hits the surface. For example, a subsurface dipole (15 km dee, moment of $2 \times 10^5 \gamma \text{ km}^3$) was calculated (Howe and McGuire, 1974 unpublished) to backscatter about 50%–60% of the incident flux into Sectors I and II in a 10γ external field. Such a remnant field would have a strength of 60γ at the lunar surface, falling off to less than 0.1γ at 100 km orbital altitude. Such scattering areas are distinguishable from an area of adiabatic mirroring by the more random pitch angle distribution of returning electrons. Sector II (45° – 90°) will show less than 100% returning flux, while Sector I (0° – 45° , which requires stronger scattering to mirror) shows a significant number of returning electrons. For the case of purely adiabatic mirroring, all electrons with pitch angles above the critical value $\alpha = \sin^{-1} \sqrt{B/B_m}$ will mirror back to the satellite, while all electrons with smaller pitch angles impact the lunar surface. This would require the flux ratio between Sector II/Sector III to increase to unity before any mirrored flux would appear in Sector I. We, therefore, are provided with a criteria for distinguish-

ing between mirroring by large (> 100 km for 14 keV electrons) areas of relatively small (0.1 to 10γ) uniform surface fields, and scattering by one or more areas of more intense magnetization confined to areas smaller than the spatial resolution element defined by the electron gyro radius and telemetry interval.

Computer simulations of flux versus pitch angle distributions to be expected from various simple surface field sources, such as a subsurface dipole, using direct force equation trajectory calculations in various assumed field configurations indicate that in some cases the particular pitch angle distribution observed from a source region can be matched to a unique calculated distribution to deduce the size, depth and configuration of the sources.

Repeated observation of the same region under different orientations of the external field provides information as to the direction of the surface field. Since the surface and external fields add vectorially, reversing the sign of the external field component greatly changes the resulting total field to which the electron scattering is sensitive. Adiabatic scattering, in particular, will occur in a region when the external field is parallel to the surface field and vanish entirely for the opposite orientation of the external guiding field, since the surface field now provides a net decrease in the total field at the surface, given by

$$B_{\text{surf}} = |\bar{B}_0 + \bar{B}_{\text{rem}}| < |\bar{B}_0| < B_m \text{ (Eqn. (1)) for all } \alpha\text{'s.}$$

Only regions where the lunar field component exceeds twice the external field value will mirror electrons under all external field orientations. Repeated observations under various external magnetic/plasma conditions also provide a means of distinguishing permanent 'fossil' surface magnetism from areas of induced magnetic response to solar wind flow, etc. (Schubert and Lichtenstein, 1974).

The potential utility of this electron scattering technique for generation of maps of lunar surface remnant magnetism is illustrated in Figure 2, which is a plot of electron backscattered intensity observed in Sector II (upper group) and Sector I (lower group) for four orbital passes across the Van de Graaff region. Each trace is displaced 50% in vertical scale for legibility. Portions of data for which return flux is less than 25% are deleted for legibility. The ground track is displaced about 30 km per orbit by lunar rotation. The pattern of return from areas crossed by the ground track can be seen to evolve as it is displaced from orbit to orbit. Evidence of numerous nonadiabatic scattering centers is seen, perhaps surrounded by areas of adiabatic scattering visible in Sector II. The scattering centers run together between 140° – 175° E. Only a single isolated area of scattering is observed east of 150° W (along these particular ground tracks).

Computer programs can be used to project the ambient magnetic field lines observed at the PFS satellite by the on-board magnetometer to their intersection point with the lunar surface. Such programs have been written to provide mapping of any areas of surface magnetic enhancement sufficient to produce detectable electron return fluxes from areas which underlie the PFS orbits and for better than 100 km to either side (during times of sufficient north–south external field component). Such mapping may

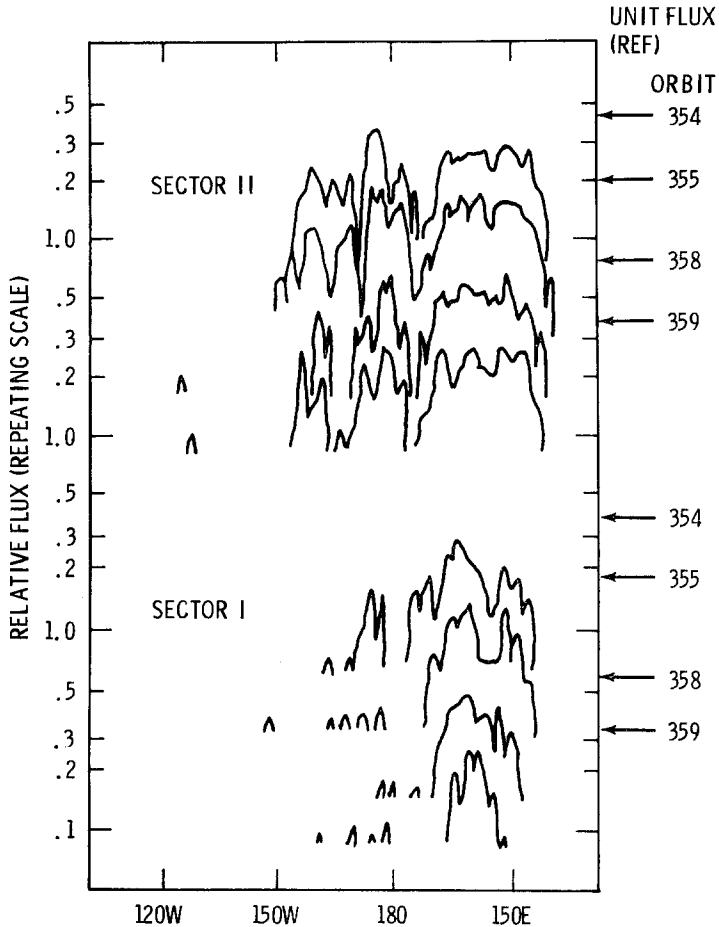


Fig. 2. Relative flux profiles for four orbits of PFS-1 showing the gradual evolution of several areas of return from intense surface magnetism as the projected orbit ground track precesses.

be done using data in the solar wind and plasma sheet, as well as in the high latitude magnetotail, thus avoiding one of the major limitations on direct analysis of the on-board magnetometer data itself. As well as providing coverage of regions not overflowed while in the high-latitude magnetotail, this also provides a means of comparing data taken in the solar wind with data over the same point in magnetotail or plasma void to detect the degree of compression or other interaction of the surface magnetism with the flow of the solar wind. For each point at which electron sector flux values are available, the calculated intersection point of the external field with the lunar surface is used to sort that point into 2×2 degree bins according to location in lunar latitude and longitude, and the presence or absence of scattered electrons from this surface location is noted. Accumulated observations from each bin are then printed out as a series of matrices, each element of which is the frequency of observation from that

point of return fluxes exceeding a specified ratio

$$[R = \text{flux (down)}/\text{flux (return)}]$$

as a function of external field orientation (in or out of the lunar surface). When many orbits of data are analyzed in this way, magnetized surface regions which consistently scatter electrons should stand out in the resulting surface maps.

2. Preliminary Results

A. DIRECT OBSERVATION ON SUCCESSIVE ORBITS

Several periods of data from both PFS-1 and PFS-2 have been visually screened for obvious areas of electron return in the raw orbital data plots. The orbits of data presented in Figure 2, for example, were selected from a series of passes (orbits 354–359, Sept. 3, 1971) over the Van de Graaff region at an altitude increasing from about 90 km at 120° W to about 140 km at 140° E. The Moon was in the southern lobe of the high latitude tail and the (external) magnetic field was quiet and anti-Sunward (B out from the lunar surface) with $B_x \sim -10\gamma$, $B_y = B_z \sim 0$ in solar ecliptic coordinates. Therefore, the C5 (14 keV electrons) pitch angle Sectors I and II were looking toward the lunar surface. The Sectors III and IV, looking away from the surface and along field lines which extended into the distant magnetotail, measured an unusually large and steady flux of ambient 14 keV electrons moving toward the earth. These electrons were produced by an earlier solar flare and moved along interplanetary field lines which reconnected far downstream at the magnetopause with high latitude tail field lines. The return electron flux in Sector II is mostly the adiabatically scattered component, due to large (>100 km) scale uniform fields of up to 10γ between the PFS and the lunar surface, while the flux in Sector I is mostly a non-adiabatically scattered component due to numerous regions of smaller scale (<50 km) fields well in excess of 20γ . Similar results are noticeable in scans of raw data from series of passes over other regions of the Moon, both back and front side.

TABLE I

Locations of areas of lunar surface magnetism found from direct examination of successive orbits for electron mirroring

longitude	latitude
55° W	16° S
14° W	7° S
50° W	10° S
42° W	10° S
153° W	0° S
111° E	10° N
169° E	6° N

As well as providing independent verification of the location of magnetic anomalies reported by the UCLA magnetometer group near the crater Van de Graaff with PFS-1 and near 149° E and 165° E (8° N) with PFS-2 data, this method has been used to locate previously unreported areas of remnant magnetism on both the front and back sides of the Moon. Locations of several are listed in Table I.

B. MAPPING OF ACCUMULATED AVERAGES

Preliminary maps of regions of surface magnetism have been generated from PFS-2 data with about 40% coverage from 10° N to 15° S (Figures 3–6). Refinement of the techniques and use with all of the data available from PFS-1 and PFS-2 should allow essentially complete coverage of the lunar surface from 35° N to 35° S, with some coverage to latitudes above 40°. We present maps outlining areas of greater than 30% probability of observing return electron fluxes exceeding various threshold ratios in steps of less than 10% to greater than 70%, for external field orientations into or out of the lunar surface. A reflection coefficient of 10% implies (Equation (1)) an approximate B_s/B_0 ratio of 1.01, or a surface field averaged over the ~ 100 km probed area of 0.1γ in a typical ambient field of 10γ (for the case of orientation parallel to the external field). Successively higher reflection coefficients imply appropriately higher minimum average surface field. In each map, the areas of most consistent returning

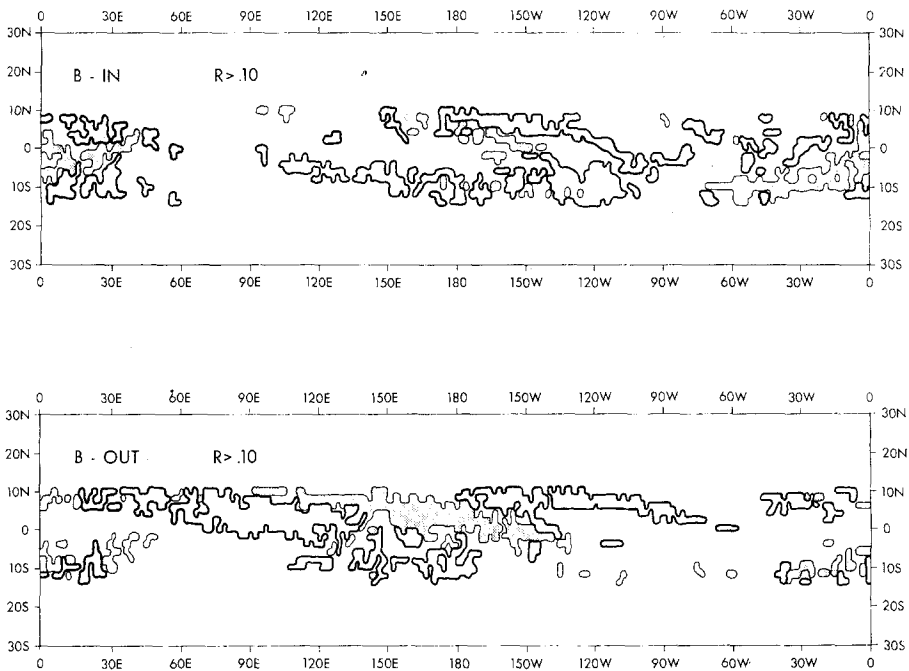


Fig. 3. Preliminary mapping of lunar surface magnetism sufficient to return at least 10% of the incident electron flux (fine outline and shaded area). Regions observed to lack any return flux (non-magnetic) are also shown as a heavy outline.

electron observation are shaded to highlight the regions of strongest (or most spatially pervasive) magnetism.

Figure 3 shows the resulting maps for the most sensitive threshold used, a reflection coefficient of 10%. In addition to showing the areas of observed occurrence of surface magnetism exceeding this minimum threshold (fine line outlines and shaded regions), we also show (as a heavy line outline) those regions for which data were obtained showing no reflection at all above this threshold. Areas not included within either outline on these maps either had an insufficient number of observations (less than 3) to be considered reliable, or were observed to have only sporadic (less than 30% of observations) electron return (which would possibly be due to induced transients or other effects, rather than a permanent surface field). Note that areas which fall within either fine or heavy outlines on both maps (*B*-in and *B*-out, referring to the sense of the external magnetic field with respect to the lunar surface) may, therefore, be placed within one of the four following categories:

(1) Return flux ratio less than 10% (heavy outline) on both maps – these areas must lack significant magnetism of any orientation; not exceeding an average of $0.1\text{--}0.3\gamma$ over the area probed ($\sim 100\text{ km}$), nor exceeding $1\text{--}3\gamma$ over any 10% of that area, nor exceeding $10\text{--}30\gamma$ over any 1% of that area.

(2) *R* more than 10% (fine outline) on both maps – these areas must have sufficient magnetism to scatter electrons regardless of orientation; either exceeding 20γ (twice

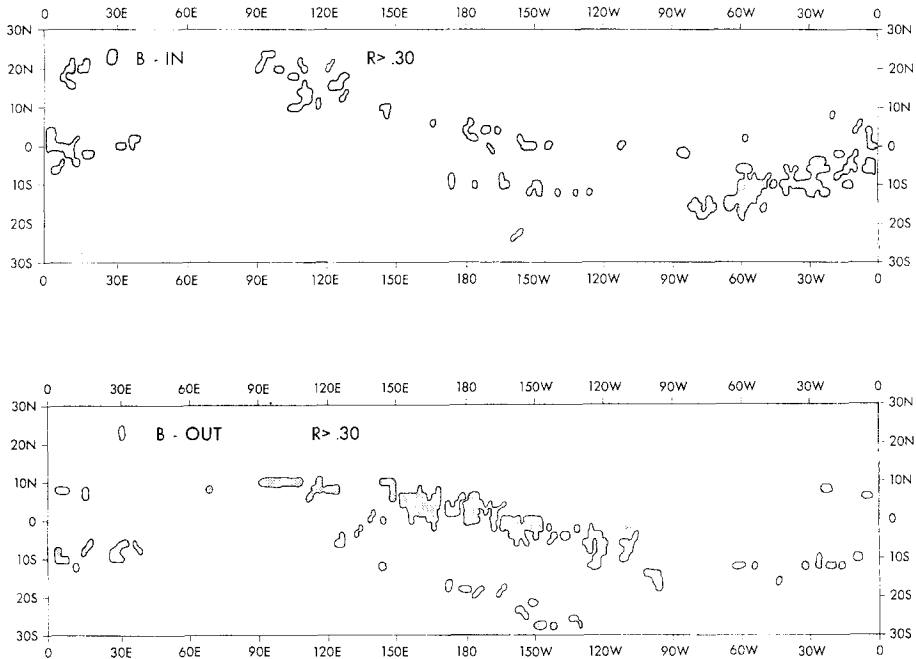


Fig. 4. Preliminary maps of lunar surface magnetism sufficient to return at least 30% of the incident electron flux.

average 10γ external field) if oriented radially in or out of the surface, or else with a horizontal component in excess of 0.3γ averaged over the entire area, or 3γ averaged over 10% of the area, etc. This case will include the areas of non-adiabatic scattering from smaller regions of very intense ($> 50\gamma$) field.

(3) R more than 10% for B -in, less than 10% for B -out – these areas would have a field oriented mostly radially into the surface, exceeding an average of 0.1γ over the area probed (but less than the fields necessary for category 2).

(4) R more than 10% for B -out, less than 10% for B -in – these areas would have a field oriented mostly radially out from the lunar surface, exceeding an average of 0.1γ over the area probed (but less than the fields necessary for category 2).

The coverage is incomplete, as only a small portion of the data available, from PFS-2 only, was used.

Figure 4 shows the same sort of maps for a less sensitive threshold, a reflection coefficient of 30%. Areas of magnetism appearing on these maps can also be grouped into any of the last three categories described above, with the indicated surface fields increased by a factor of three. The preliminary maps shown include additional areas not on the maps in Figure 3, due to inclusion of some additional data including a few days from the more highly inclined orbit of PFS-1. Although still very incomplete, even these preliminary maps indicate that surface magnetism appears to be a common feature over all areas of the Moon which were covered, front side as well as back. The

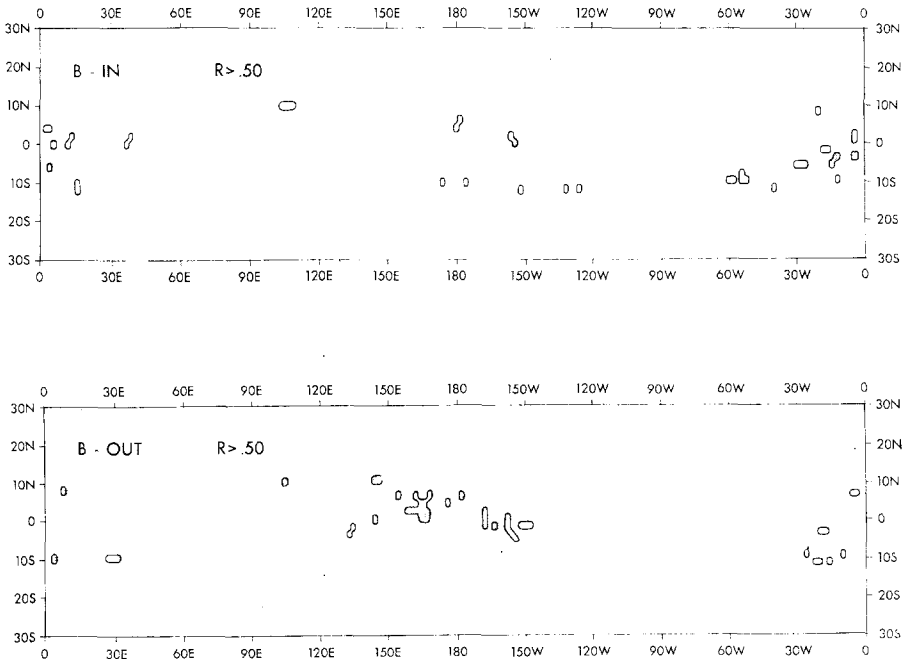


Fig. 5. Preliminary maps of lunar surface magnetism sufficient to return at least 50% of the incident electron flux.

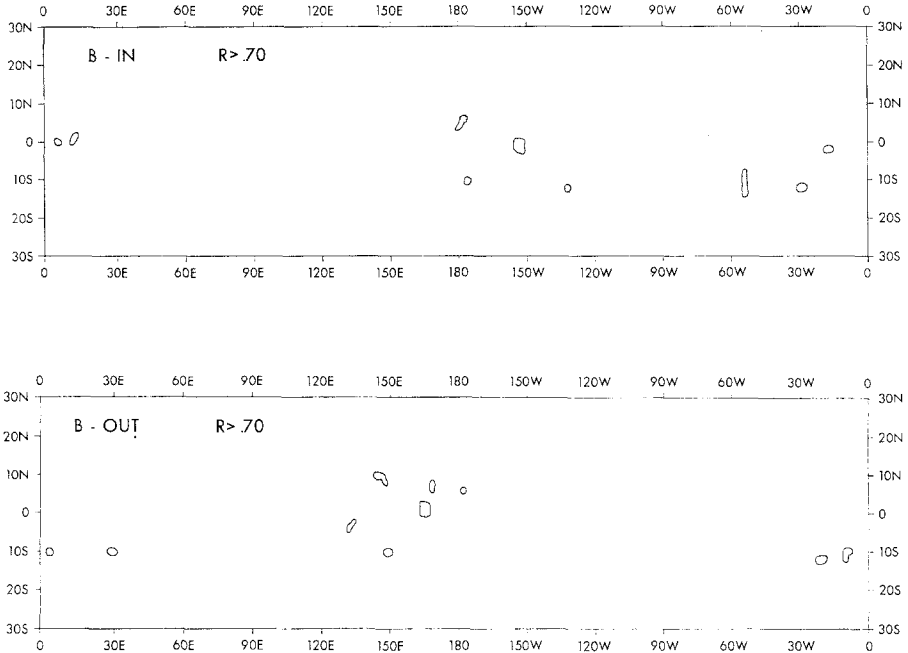


Fig. 6. Preliminary maps of lunar surface magnetism sufficient to return at least 70% of the incident electron flux.

apparent dominance of *B*-in on the front side and *B*-out on the back is possibly only a reflection of the most frequent orientation of the ambient field during the times coverage of each region was obtained. Note the extensive, somewhat spotty, occurrence of areas of magnetism across the southern end of Procellarum and the central highlands.

Figures 5 and 6 are similar in content to Figure 4, with higher reflection coefficients of 50% and 70% to show only the regions of strongest and most pervasive surface field. The coverage is incomplete, using only the smaller data set used for Figure 3. No coverage of the intense areas near Van de Graaff and southern Procellarum was included, although both would have shown up strongly on such maps (based on direct examination of data, see Figure 2).

C. COMPARISON WITH ORBITAL MAGNETOMETER MAPS

Comparison of these results with maps of magnetic field components observed from orbit by the UCLA magnetometer group indicates a general agreement as to the existence of most large features found in the areas where the two mappings presently overlap. Detailed configuration of the regions observed shows quite a bit of difference, in the direction of more detail and confusion in the primarily surface mappings we obtain. This seems consistent with the magnetometer results obtained with the PFS-2 data, which show two rather different maps across the same region when using data

from lower versus higher altitudes. These two magnetometer maps display the same tendency toward greater profusion of small scale, but more intense, magnetic features at lower altitudes which mostly merge together or disappear altogether in the higher altitude data.

This is further supported by those single passes having sufficient flux levels to give good counting statistics (such as shown in Figure 2), which consistently show features with dimensions at the limit of resolution or with the appearance of a running together of several sources smaller than the resolution available. During the final few orbits of PFS-2, the (satellite) magnetometer passed through a few isolated areas of magnetism, small at higher altitudes, one of which increased to greater than 20γ at the very lowest altitudes (of less than a few kilometers). This feature was also clearly visible in the electron data for many orbits, as well as several similar features, two of which had also begun to show in the lowest altitude magnetometer data. That these features were easily observable in the electron data well before the altitude became low enough for the magnetometer to respond, and then were confirmed by direct magnetometer penetrations, provides a strong confirmation of the ability of this method to probe for surface fields from altitudes well above measureable residuals seen by an orbiting magnetometer. Further examination of these last few orbits will yield valuable tests of the extent of the ability of the electron measurements to predict the lower altitude fields later sampled directly by the magnetometer.

3. Conclusions

We have presented the first results of a new method for mapping regions of lunar surface magnetism by remote sensing from an orbiting spacecraft. Rather than using direct measurement by a magnetometer, which must physically pass through the fields to be measured, this method uses electron data as a function of angle with respect to the ambient magnetic field lines. Examination of such data for occurrence of electron fluxes from directions forbidden except for 'mirroring' above the lunar surface by local magnetic fields will provide a mapping of regions of occurrence of such fields. Use of the on-board vector magnetometer measurements of the ambient magnetic field orientation allows accurate projection of such mapping onto the lunar surface. The ambient electrons provide, in effect, a probe along the ambient magnetic field lines down to the lunar surface for remote sensing of the presence of surface fields. This probe, unlike direct measurement by the magnetometer, does not require low altitude (to pass through the low altitude fields being measured) or a very stable ambient field (to allow subtraction from the small lunar fields being measured).

Preliminary maps of the lunar surface magnetic areas lying under the (Apollo 16) PFS-2 orbit have been generated, obtaining 40% coverage from partial data to demonstrate feasibility of the technique. As well as providing independent verification of areas such as Van de Graaff already discovered in the magnetometer data, these maps reveal many previously unreported areas of surface magnetism.

Further refinement of the programs in use, when applied to the full body of avail-

able PFS-1 and 2 electron data, are expected to provide complete mapping of the lunar surface for areas of magnetization up to latitudes of 35° to 40° , with resolution of ~ 50 km.

Development of additional programs for detailed study of high resolution, real time, data at lower electron energies should provide resolution of selected areas of surface magnetism down to a kilometer scale. Analysis of exact angular distribution of the return electron fluxes is also expected to yield data on the magnitude, orientation, and depth below the surface of the sources of observed magnetism.

The technique is seen as a powerful addition to, rather than a replacement of, the existing magnetometer techniques for such mapping. Much additional information regarding the orientation and variation with altitude of the magnetic regions can be obtained by correlated analysis of both the electron return and vector magnetometer measurements at orbital altitude, the two techniques providing each other with directly complementary measurements at the satellite and along the ambient field lines to the surface.

Acknowledgments

The work was partially supported by NASA Contract NAS 9-10509. Magnetic field data at the satellite were provided by Dr P. J. Coleman and his co-investigators from the on-board magnetometer experiment. We are particularly grateful to Dr C. T. Russell for many helpful discussions, particularly of comparisons with the corresponding magnetometer mappings and the final PFS-2 orbits of very low altitude data.

References

- Anderson, K. A. and Lin, R. P.: 1969, *J. Geophys. Res.* **74**, 3953.
- Anderson, K. A., Chase, L. M., Lin, R. P., McCoy, J. E., and McGuire, R. E.: 1972, *J. Geophys. Res.* **72**, 4611.
- Anderson, K. A., Howe, H. C., Lin, R. P., McGuire, R. E., Chase, L. M., and McCoy, J. E.: 1974, *Lunar Science V, Abstracts*, 18.
- Coleman, P. J., Lichtenstein, B. R., Russell, C. T., Sharp, L. R., and Schubert, G.: 1972, *Geochim. Cosmochim. Acta* **36**, 2271.
- Dolginor, Sh. Sh., Eroshenko, E. G., Zhuzgov, L. N., and Pushkov, N. V.: 1966, *Dokl. Akad. Nauk SSSR* **170**, 574-577.
- Dyal, Palmer, Parkin, Curtis W., and Cassen, Patrick: 1972, *Geochim. Cosmochim. Acta, Suppl.* **3**, **36**, 2287.
- Howe, Herbert C., Lin, R. P., McGuire, R. E., and Anderson, K. A.: 1974, *Geophys. Res. Letters* **1**, 101.
- Schubert, G. and Lichtenstein, B. R.: 1974, *Rev. Geophys. Space Sci.* **12**, 592-626.
- Sharp, L. R., Coleman, P. J., Jr., Lichtenstein, B. R., Russell, C. T., and Schubert, G.: 1973, *The Moon* **7**, 322.
- Sonett, C. P., Colburn, D. S., Currie, R. G., and Mihalov, J. D.: 1967, in R. L. Carovillano, J. F. McClay and H. F. Radoski (eds.), *Physics of the Magnetosphere*, D. Reidel, Dordrecht, pp. 461-484.
- Strangway, D. W., Larson, E. E., and Pearce, G. W.: 1970, *Geochim. Cosmochim. Acta, Suppl.* **1**, **34**, 2435.
- Van Allen, J. A. and Ness, N. F.: 1969, *J. Geophys. Res.* **74**, 71.